




Passing through resonance of the unbalanced rotor with self-balancing device

Olga Drozdetskaya · Alexander Fidlin 

Received: 1 July 2021 / Accepted: 6 October 2021 / Published online: 24 October 2021
© The Author(s) 2021

Abstract The slow dynamics of unbalanced rotors with a passive self-balancing system are investigated considering the interaction of the mechanical system with a limited power engine. The slow dynamics equations are obtained using the averaging technique for partially strongly damped systems. Stationary system configurations, different types of nonstationary solutions while passing through resonance, and areas of stability and attraction are investigated.

Keywords Self-balancing · Averaging · Nonlinear resonance · Sommerfeld effect

1 Introduction

Self-balancing systems were invented at the beginning of the twentieth century [15]; they allow for the complete compensation of unbalance at critical rotor speeds and can be used in mechanical systems with variable imbalance, such as washing machines and laboratory centrifuges. Most analytical studies of self-balancing systems focus on the existence and stability of compensating solutions, with the rotor speed being assumed to be constant and the interaction of the mechanical system without considering the drive ([1, 6, 12, 14]).

Experimental studies of the dynamics of a simple self-balancing system were also performed at a given constant rotor drive speed [7]. However, the vibrations of even simpler mechanical systems can have a strong influence on drive rotation, causing the system to be captured into resonance and hindering it from reaching operating speed (see [2, 3]). The existence of nonsynchronous motions in autobalancing systems near the resonant rotation speed considering the engine characteristic was described in [13]. It was shown that at a certain speed near resonance, the balancing masses no longer synchronize with the rotor and remain instead at a frequency just below the resonance rate. This balancing mass behavior leads to a strong increase in the system vibration amplitude and in some cases to a strong modulation. Similar solutions have also been mentioned in works by other authors, e.g., when investigating the effect of damping on the speed of synchronization of balancing masses [5], in studies of balancing quality by increasing the number of balancing masses and/or their raceways [8, 9], and studies of self-balancing in a disk mounted on a flexible cantilever shaft [11]. In most of these publications, however, these solutions were observed assuming a given or constant rotor speed, which in most cases is not an adequate assumption when studying the passage through resonance. Thus, these phenomena have not yet been systematically studied and explained. The objective of this paper is to consider the slow dynamics of a simple self-balancing system while passing through resonance, considering interactions with limited power

O. Drozdetskaya · A. Fidlin (✉)
Karlsruhe Institute of Technology, Kaiserstr. 10, 76131
Karlsruhe, Germany
e-mail: alexander.fidlin@kit.edu

engines, the study of types of possible solutions, and the estimation of areas of their existence, stability and attraction.

The paper is structured as follows. Section 2 presents a minimal plane model of an unbalanced rotor with a self-balancing system and its equations of motion. In Sect. 3, the slow dynamics equations of the considered system are derived. Stationary solutions of the system are considered in Sect. 4. Section 5 presents an overview of the types of transient processes occurring in the system. Section 6 investigates the regions of attraction of different types of solutions taking into account the variation in the engine characteristic and the initial rotor speed. Section 7 is devoted to investigating the stability of the transient resonance solution. The most important results of this study are summarized in Sect. 8.

2 The simplest model of an unbalanced rotor with a pendulum-type self-balancing device

Consider the system in Fig. 1a that represents the simplest model of an unbalanced rotor with a self-balancing device driven by a limited power engine.

A rotor of mass M and moment of inertia J_r is elastically suspended by a spring-damper element of stiffness c and damping β_r . The center of mass of the rotor has an offset e relative to the axis of rotation. Two pendulum balancers of mass m , mass moment of inertia J_p and length r are mounted coaxially with the main rotor. There is viscous damping between the main rotor and the pendulum balancers (damping coefficient β_r). The rotor is excited by a limited power engine.

Equations of motion and the nondimensional parameters The equations of motion for this system can be written as follows:

$$(M+2m)\ddot{x} + \beta_r \dot{x} + c_r x = Me(\dot{\phi}^2 \cos \phi + \ddot{\phi} \sin \phi) + mr \sum_{i=1}^2 \left((\dot{\phi} + \dot{\psi}_i)^2 \cos(\phi + \psi_i) + (\ddot{\phi} + \ddot{\psi}_i) \sin(\phi + \psi_i) \right), \tag{1}$$

$$(J_r + Me^2)\ddot{\phi} - \beta_\phi(\dot{\psi}_1 + \dot{\psi}_2) = T_{mot} + Me\ddot{x} \sin \phi, \tag{2}$$

$$(J_p + mr^2)(\ddot{\psi}_i + \ddot{\phi}_i) + \beta_\phi \dot{\psi}_i = mr\ddot{x} \sin(\phi + \psi_i), \quad i = 1, 2. \tag{3}$$

Equation (1) describes the displacement of the whole system, Eq. (2) describes the rotational angle of the rotor, and Eq. (3) describes the rotation of the pendulum balancers.

The simplest case of linearized static characteristics is used to describe the engine torque:

$$T_{mot} = U(\omega^* - \dot{\phi}). \tag{4}$$

Here, parameter U is the slope of the engine characteristic, and parameter ω^* is the nominal rotation speed of the engine.

New coordinates are introduced to simplify further analysis: mean phase shift

$$\psi = \frac{\psi_1 + \psi_2}{2} \tag{5}$$

and the angle between the pendulums (s. Fig. 1b)

$$\delta = \psi_1 - \psi_2. \tag{6}$$

The dimensionless parameters are introduced

$$\begin{aligned} M^* &= M + 2m; \quad k^2 = \frac{c_r}{M^*}; \quad \tau = kt; \quad \xi = \frac{M^*}{mr}x; \\ \sigma &= \frac{\beta_c}{2kM^*} = \mathcal{O}(1); \\ s &= \frac{Me}{mr}; \quad \varepsilon = \frac{1}{1 + J_r/Me^2} \ll 1; \\ b_r &= \frac{\beta_r \varepsilon}{kMe^2} = \mathcal{O}(1); \quad w = \frac{mr}{M^*e}; \quad \lambda = \frac{\omega^*}{k}; \\ u &= \frac{U}{kMe^2}; \quad p = \frac{1}{1 + J_p/mr^2}; \\ b_p &= \frac{\beta_r p}{kmr^2} = \mathcal{O}(1); \quad \mu = p \frac{m}{M^*} = \mathcal{O}(\varepsilon). \end{aligned} \tag{7}$$

The equations of motion are rewritten in the form:

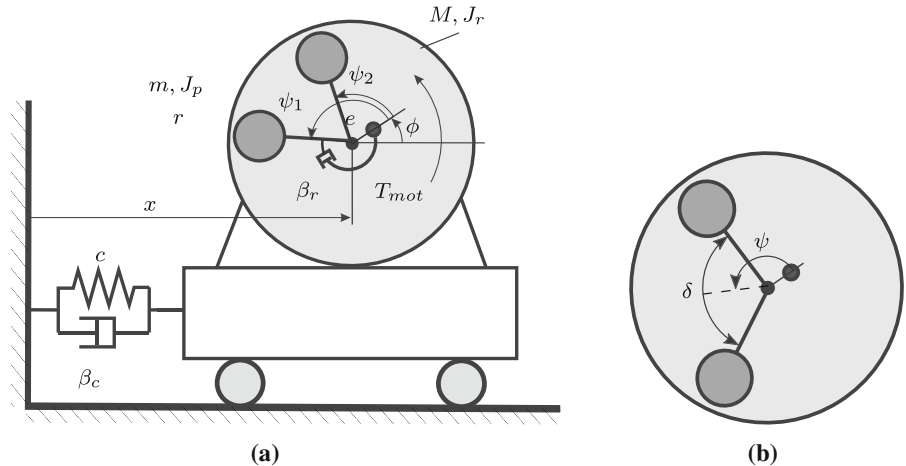
$$\xi'' + 2\sigma\xi' + \xi = f_\xi(\phi, \phi', \phi'', \psi, \psi', \psi'', \delta, \delta', \delta''), \tag{8}$$

$$\phi'' - 2b_r\psi' = \varepsilon f_\phi(\phi, \phi', \xi''), \tag{9}$$

$$\psi'' + (b_p + 2b_r)\psi' = \varepsilon f_\psi(\xi'', \phi, \phi', \psi, \delta), \tag{10}$$

$$\delta'' + b_p\delta' = \varepsilon f_\delta(\xi'', \phi, \phi', \psi, \delta), \tag{11}$$

Fig. 1 **a** Model of a rotor with a self-balancing device; **b** new coordinates



where

$$\begin{aligned}
 f_{\xi}(\phi, \phi', \phi'', \psi, \psi', \psi'', \delta, \delta', \delta'') &= s(\phi'^2 \cos \phi + \phi'' \sin \phi) + \\
 &+ \left(\phi' + \psi' + \frac{\delta'}{2}\right)^2 \cos\left(\phi + \psi + \frac{\delta}{2}\right) \\
 &+ \left(\phi'' + \psi'' + \frac{\delta''}{2}\right) \sin\left(\phi + \psi + \frac{\delta}{2}\right) \quad (12) \\
 &+ \left(\phi' + \psi' - \frac{\delta'}{2}\right)^2 \cos\left(\phi + \psi - \frac{\delta}{2}\right) \\
 &+ \left(\phi'' + \psi'' - \frac{\delta''}{2}\right) \sin\left(\phi + \psi - \frac{\delta}{2}\right),
 \end{aligned}$$

$$\varepsilon f_{\phi}(\phi, \phi', \xi'') = \varepsilon(w\xi'' \sin \phi + u(\lambda - \phi')), \quad (13)$$

$$\begin{aligned}
 \varepsilon f_{\psi}(\xi'', \phi, \phi', \psi, \delta) &= \mu\xi'' \sin(\phi + \psi) \cos\left(\frac{\delta}{2}\right) - \varepsilon f_{\phi}, \quad (14)
 \end{aligned}$$

$$\varepsilon f_{\delta}(\xi'', \phi, \phi', \psi, \delta) = 2\mu\xi'' \sin\left(\frac{\delta}{2}\right) \cos(\phi + \psi). \quad (15)$$

It is important to note that all damping coefficients σ , b_p and b_r are not small.

3 Asymptotic analysis

To derive equations describing the slow dynamics of the autobalancing system, the averaging method for partially strongly damped systems is used. The method was proposed in [4], and its mathematical motivation is described in [3] and [2]. The main idea of the method is to separate strongly and weakly damped variables and

to consider only the slow dynamics of weakly damped variables. Strongly damped variables are replaced by their stable stationary or periodic solutions on the slow manifold.

First, consider Eqs. (9)–(11). The variable transformation is introduced

$$\tilde{\psi} = \frac{\psi' + (b_p + 2b_r)\psi}{b_p + 2b_r}, \quad (16)$$

$$\psi = \tilde{\psi} + \alpha, \quad (17)$$

$$\tilde{\delta} = \frac{\delta' + b_p\delta}{b_p}, \quad (18)$$

$$\delta = \tilde{\delta} + \beta, \quad (19)$$

$$\omega = \phi'. \quad (20)$$

The equations can be written in the form

$$\phi' = \omega, \quad (21)$$

$$\omega' = \varepsilon f_{\phi} - 2b_r(b_p + 2b_r)\alpha, \quad (22)$$

$$\tilde{\psi}' = \frac{\varepsilon f_{\psi}}{b_p + 2b_r}, \quad (23)$$

$$\alpha' = -(b_p + 2b_r)\alpha - \frac{\varepsilon f_{\psi}}{b_p + 2b_r}, \quad (24)$$

$$\tilde{\delta}' = \frac{\varepsilon f_{\delta}}{b_p}, \quad (25)$$

$$\beta' = -b_p\beta - \frac{\varepsilon f_{\delta}}{b_p}. \quad (26)$$

Variables α and β are strongly damped and can be replaced in the first order approximation by the stationary solutions of Eqs. (24) and (26) respectively:

$$\alpha_0 = -\frac{\varepsilon f_{\psi}}{(b_p + 2b_r)^2}, \quad (27)$$

$$\beta_0 = -\frac{\varepsilon f_{\delta}}{b_p^2}. \tag{28}$$

So in the first-order approximation

$$\psi = \tilde{\psi} + \mathcal{O}(\varepsilon), \tag{29}$$

$$\delta = \tilde{\delta} + \mathcal{O}(\varepsilon). \tag{30}$$

Then, Eq. (8) can also be rewritten as

$$\begin{aligned} \xi'' + 2\sigma\xi' + \xi = & \omega^2 \left(s \cos \phi + \cos \left(\phi + \tilde{\psi} + \frac{\tilde{\delta}}{2} \right) \right) \\ & + \omega^2 \cos \left(\phi + \tilde{\psi} - \frac{\tilde{\delta}}{2} \right) + \mathcal{O}(\varepsilon). \end{aligned} \tag{31}$$

Then, the first approximation describing a purely forced solution can be easily found explicitly:

$$\begin{aligned} \xi_p = & \hat{\xi}_p (1 - \omega^2) \left(s \cos(\phi) + \cos \left(\phi + \tilde{\psi} + \frac{\tilde{\delta}}{2} \right) \right. \\ & \left. + \cos \left(\phi + \tilde{\psi} - \frac{\tilde{\delta}}{2} \right) \right) \\ & + 2\hat{\xi}_p \sigma \omega \left(s \sin(\phi) + \sin \left(\phi + \tilde{\psi} + \frac{\tilde{\delta}}{2} \right) \right. \\ & \left. + \sin \left(\phi + \tilde{\psi} - \frac{\tilde{\delta}}{2} \right) \right), \hat{\xi}_p = \frac{\omega^2}{(1 - \omega^2)^2 + 4\omega^4 \sigma^2}. \end{aligned} \tag{32}$$

Variable transformation

$$\xi = \xi_p + \rho \sin \kappa \tau + \nu \cos \kappa \tau, \tag{33}$$

$$\xi' = \xi'_p + \rho \kappa \cos \kappa \tau - \nu \kappa \sin \kappa \tau$$

$$-\sigma(\rho \sin \kappa \tau + \nu \cos \kappa \tau), \tag{34}$$

$$\kappa = \sqrt{1 - \sigma^2}, \tag{35}$$

leads to a system of two differential equations of the first order with strongly damped variables:

$$\rho' = -\sigma\rho + \mathcal{O}(\varepsilon), \tag{36}$$

$$\nu' = -\sigma\nu + \mathcal{O}(\varepsilon). \tag{37}$$

Stationary solutions for variables ρ and ν have a magnitude order of ε , and they can be ignored in the first-order approximation. Finally, considering ϕ as an independent variable, the system can be written in a standard form

$$\frac{d\omega}{d\phi} = \frac{1}{\omega} \left(\varepsilon f_{\phi} + \frac{2b_r \varepsilon f_{\psi}}{b_p + 2b_r} \right), \tag{38}$$

$$\frac{d\tilde{\psi}}{d\phi} = \frac{\varepsilon f_{\psi}}{\omega(b_p + 2b_r)}, \tag{39}$$

$$\frac{d\tilde{\delta}}{d\phi} = \frac{\varepsilon f_{\delta}}{\omega b_p}. \tag{40}$$

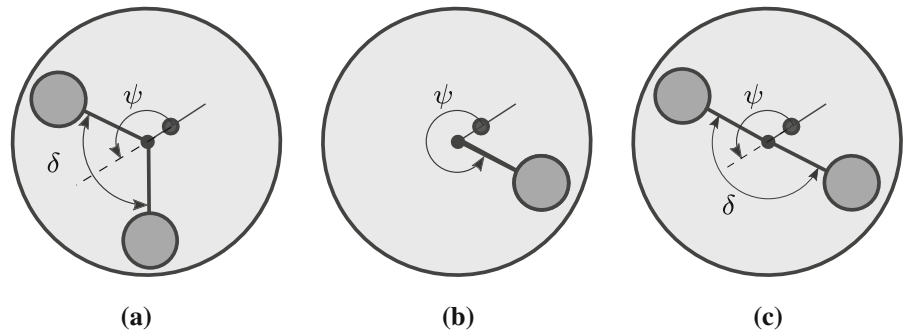
The averaged equations of the first-order approximation are

$$\begin{aligned} \bar{\omega}' = & \frac{\varepsilon b_p u (\lambda - \bar{\omega})}{\bar{\omega} (b_p + 2b_r)} - \frac{\bar{\omega}^3 B (2\mu b_r (1 + \cos \delta) + \varepsilon b_p s w)}{2(b_p + 2b_r)(A^2 + B^2)} \\ & + \frac{\bar{\omega}^3 \cos \left(\frac{\bar{\delta}}{2} \right) (A(\mu b_r s - \varepsilon w b_p) \sin \bar{\psi} - B(\mu b_r s + \varepsilon w b_p) \cos \bar{\psi})}{(b_p + 2b_r)(A^2 + B^2)}, \end{aligned} \tag{41}$$

$$\begin{aligned} \bar{\psi}' = & -\frac{\varepsilon u (\lambda - \bar{\omega})}{\bar{\omega} (b_p + 2b_r)} - \frac{\bar{\omega}^3 B (\mu b_r (1 + \cos \delta) - \varepsilon s w)}{2(b_p + 2b_r)(A^2 + B^2)} \\ & + \frac{\bar{\omega}^3 \cos \left(\frac{\bar{\delta}}{2} \right) (A(\mu s + 2\varepsilon w) \sin \bar{\psi} - B(\mu s - 2\varepsilon w) \cos \bar{\psi})}{(b_p + 2b_r)(A^2 + B^2)}, \end{aligned} \tag{42}$$

$$\begin{aligned} \bar{\delta}' = & \frac{\mu \bar{\omega}^3 \left(A \left(2 \cos \left(\frac{\bar{\delta}}{2} \right) + s \cos \bar{\psi} \right) + B s \sin \bar{\psi} \right) \sin \left(\frac{\bar{\delta}}{2} \right)}{b_p (A^2 + B^2)}, \\ A = & \bar{\omega}^2 - 1, \quad B = 2\sigma \bar{\omega}. \end{aligned} \tag{43}$$

Fig. 2 Stationary configurations of the system)



Here, $\bar{\omega}$ is the averaged rotor velocity, $\bar{\psi}$ is the averaged mean phase shift, and $\bar{\delta}$ is the averaged angle between the pendulums.

4 Stationary solutions

Equations for determining stationary solutions are obtained by setting the right-hand sides of Eqs. (41)–(43) to zero. The system has three types of stationary solutions, as shown in Fig. 2.

- 1. Compensating configuration I (see Fig. 2a)

$$\bar{\psi} = \pi, \tag{44}$$

$$\bar{\delta} = 2 \arccos\left(\frac{s}{2}\right), \tag{45}$$

$$\bar{\omega} = \lambda \tag{46}$$

With this type of solution, the pendulum balancers fully compensate for the imbalance in the main rotor, the effective center of mass of the system lies on the axis of rotation, and the rotor rotates at its nominal speed. This solution is always stable.

- 2. Coinciding configuration II (see Fig. 2b)

$$\bar{\psi} = \arctan\left(\frac{B(2A^2 + \sqrt{s^2(A^2 + B^2) - 4B^2})}{A(-4B^2 + \sqrt{s^2(A^2 + B^2) - 4B^2})}\right) \tag{47}$$

$$\bar{\delta} = 0. \tag{48}$$

In this configuration, the steady-state rotor speeds cannot be determined analytically. However, the equations can be solved, e.g., with respect to the engine parameter u , as a function of the stationary rotor speed $\bar{\omega}$:

$$u = -\frac{\omega^5 w \sigma A^2 (s^2 + 1) + B^2 (s^2 - 1) \pm \sqrt{A^2 (A^2 s^2 + B^2 (s^2 - 1))}}{s(\bar{\omega} - \lambda)(A^2 + B^2)^2}. \tag{49}$$

In this configuration, the pendulum balancers have the same angular position and, depending on the

rotor speed, can either partially compensate for the imbalance in the main rotor or intensify it. This type of solution is identical to the stationary solutions for the vibration exciter with two coaxial imbalances (see [2]). The only difference is the stability of the branches of this type of solution. In the case of the vibration exciter, there are stable branches in both the undercritical and overcritical speed ranges. However, only the branch in the undercritical range is stable for the autobalancing system. Both overcritical branches of the solution are unstable.

- 3. Opposing configuration III (see Fig. 2c)

$$\bar{\psi} = \arctan\frac{A}{B}, \tag{50}$$

$$\bar{\delta} = \pi. \tag{51}$$

Similar to the previous configuration, the stationary rotor speeds are determined indirectly by solving equations relating to the engine parameter u as a function of the stationary rotor speed $\bar{\omega}$:

$$u = \frac{\bar{\omega}^5 s \sigma w}{(\bar{\omega} - \lambda)(A^2 + B^2)}. \tag{52}$$

In this configuration, the pendulum balancers are in the counterphase and compensate for each other. This configuration is always unstable.

Figure 3 shows the dependence of stationary rotor speeds for all stationary configurations on the parameter u corresponding to the engine power for the system with the following dimensionless parameters:

$$\begin{aligned} s &= 1, \quad p = 0.99, \quad w = 0.98, \\ \lambda &= 1.51, \quad b_r = 1, \quad b_p = 1, \\ \mu &= 0.0097, \quad \varepsilon = 0.0099, \quad \sigma = 0.1. \end{aligned} \tag{53}$$

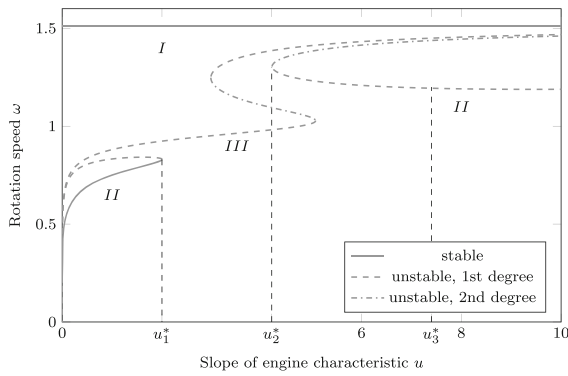


Fig. 3 Dependence of stationary rotor speeds on the bifurcation parameter u proportional to the engine characteristic slope

5 Numeric run-up simulations

Next, the results of the numerical simulations for rotor acceleration at different engine characteristic slope values and different initial conditions are considered.

Figure 4 shows the results of the run-up simulation in the case of a low value of the engine characteristic slope, which corresponds to a low-power engine. If the angular positions of the pendulums coincide at the beginning ($\delta_0 = 0$, red lines in Fig. 4), this configuration is maintained when the rotor accelerates. The system tends to achieve a stable stationary type *II* solution that corresponds to stationary capture into resonance, also known as the Sommerfeld effect [3].

If the parameter u is increased above the critical value u_1^* (see Fig. 5), the stationary solution of type *II* disappears. Instead, there is a periodic solution characterized by a very slow modulation of the rotor speed (red line in Fig. 5a). In this case, the pendulums

continue to move together as a unit, but they rotate slightly slower than the main rotor, resulting in a periodic change in the effective imbalance of the entire system. The mechanism of the emergence of this type of solution is discussed in detail in [2].

In both cases considered, the resonant solutions coexist with the stable compensating solution corresponding to the passage through resonance (see the green lines in Figs. 4 and 5).

In self-balancing systems, this solution coexists with a stable compensating solution (see the green and red lines in Fig. 5a).

If parameter u is further increased above the critical value u_3^* , the periodic solution disappears (see Fig. 6). Thus, in the case of ideal fulfillment of initial conditions $\delta_0 = 0$, the system cannot reach the compensating solution within a finite time, remaining near the unstable stationary solution of type *II* (see the red line in Fig. 6a). This scenario does not occur in practice. The slightest deviation from the initial conditions results in the system leaving the slow manifold $\delta = 0$ and tends toward a compensatory solution (the blue lines in Fig. 6).

6 Attraction areas of compensating and resonance solutions

The coexistence of several stable solutions motivates a careful analysis of their attraction areas. To geometrically interpret the attraction areas of different types of solutions, the mean phase shift $\bar{\psi}$ and the angle between the pendulums $\bar{\delta}$ are converted to the coordinates of the effective center of mass of the entire system (rotor and

Fig. 4 Evaluation of the rotor rotation speed ω **a** and the angle δ between the pendulums **b** for different values of initial angle δ_0 between the pendulums and the engine characteristics slope $u = 1.5$, ($\sigma = 0.1$)

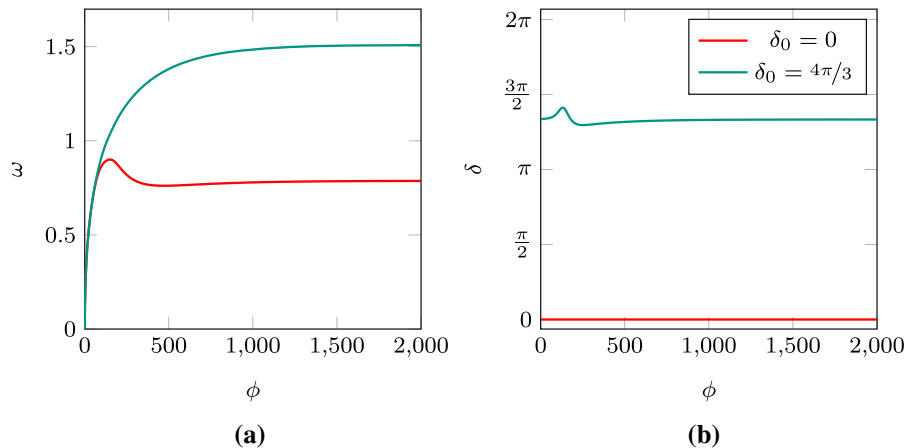


Fig. 5 Evaluation of the rotor rotation speed ω **a** and the angle δ between the pendulums **b** for different values of initial angle δ_0 between the pendulums and the engine characteristics slope $u = 4$, ($\sigma = 0.1$)

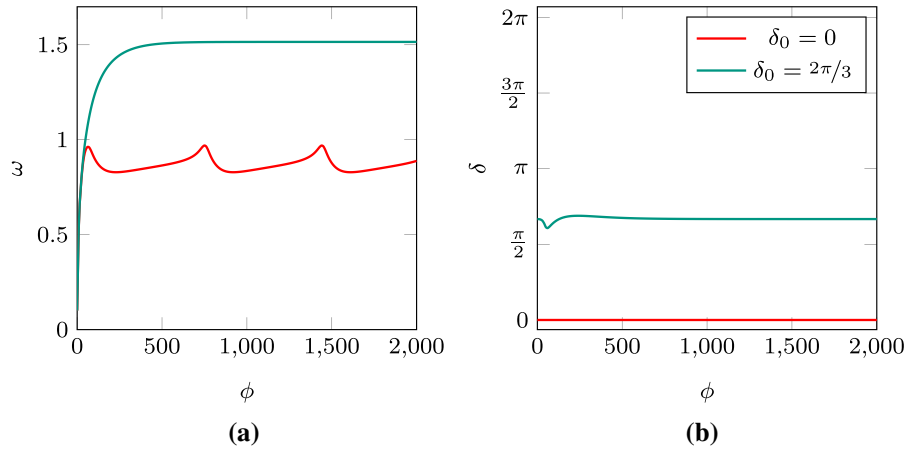
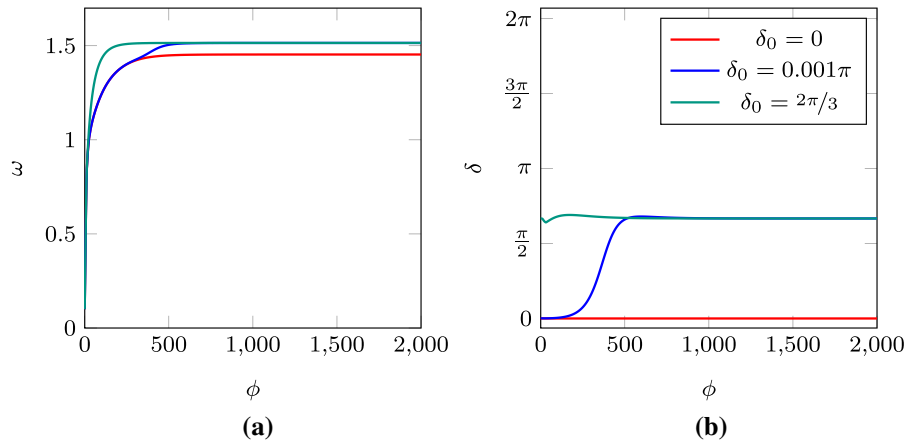


Fig. 6 Evaluation of the rotor rotation speed ω **a** and the angle δ between the pendulums **b** for different values of initial angle δ_0 between the pendulums and the engine characteristics slope $u = 9$, ($\sigma = 0.1$)



two balancing pendulums) in the corotating coordinate system:

$$\bar{\xi}_c = s + 2 \cos(\bar{\psi}) \cos\left(\frac{\bar{\delta}}{2}\right), \tag{54}$$

$$\bar{\eta}_c = 2 \sin(\bar{\psi}) \cos\left(\frac{\bar{\delta}}{2}\right). \tag{55}$$

The point with coordinates $(\bar{\xi}_c = 0, \bar{\eta}_c = 0)$ corresponds to the axis of rotor rotation. If the two balancing pendulums coincide ($\bar{\delta} = 0$), the center of mass moves in a circle whose center is displaced by dimensionless eccentricity s from the axis of rotation. If the balancing pendulums are open ($\bar{\delta} \neq 0$), the center of mass lies not on the circle but inside it.

Considering the rotor speed $\bar{\omega}$ as a third coordinate provides a three-dimensional phase space filled with phase trajectories (see Fig. 7) and three-dimensional areas of attraction (attraction volumes) of different types of solutions.

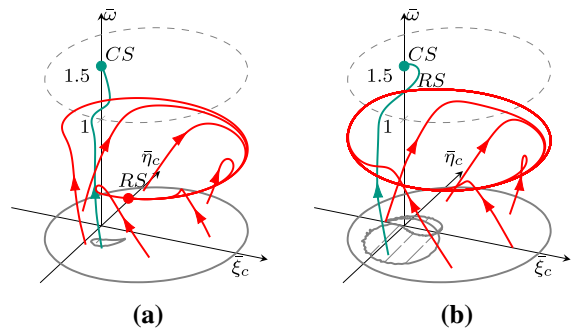
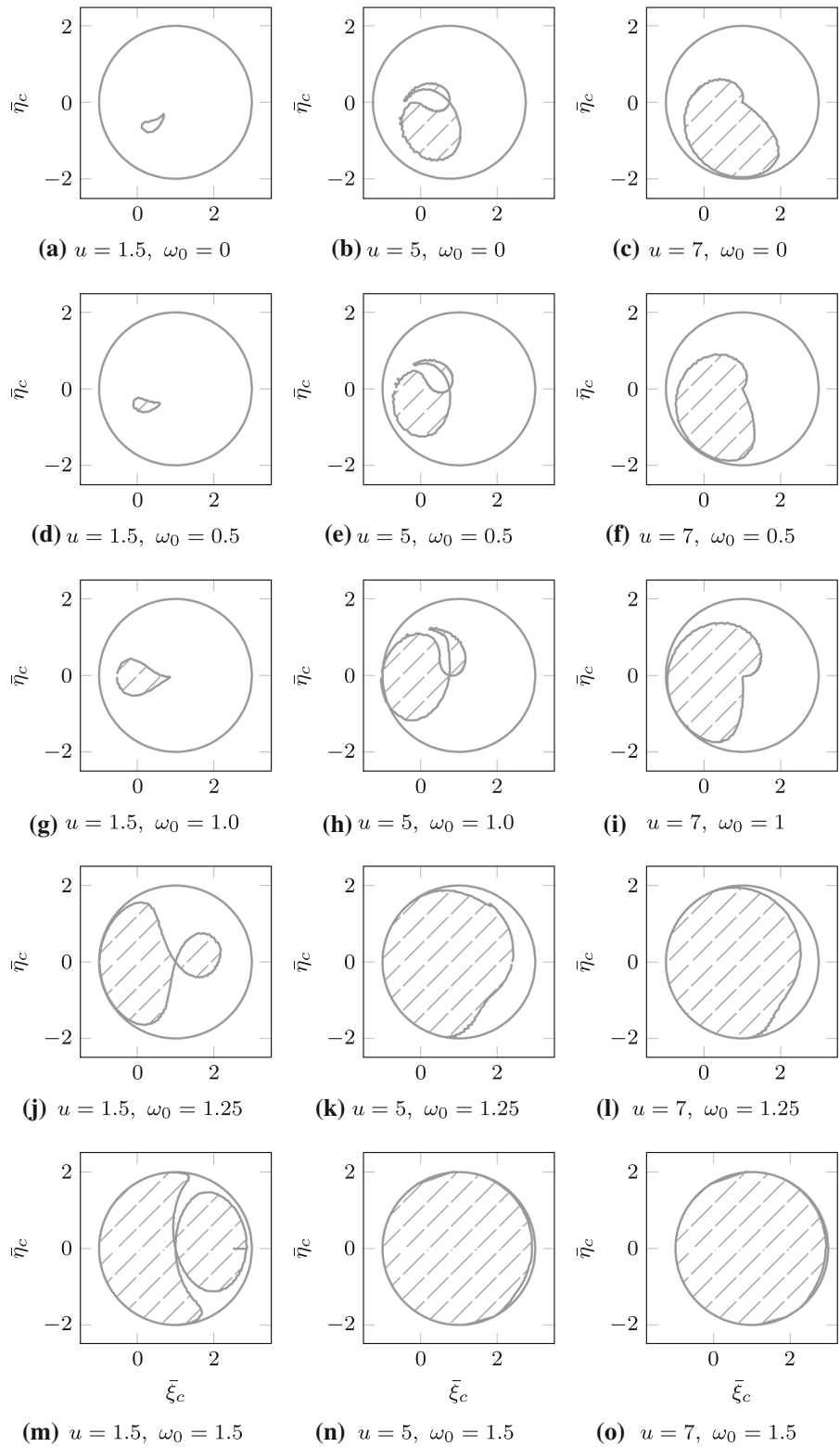


Fig. 7 Phase flow at acceleration from a resting position in cases of stationary **a** and periodic **b** resonance solutions

Figure 8 shows cross sections of the attraction areas of different solution types for different values of engine parameter u by planes corresponding to different levels of initial rotor velocity $\bar{\omega}_0$. The shaded areas correspond to the attraction area of the compensating solu-

Fig. 8 Attraction area of the compensating solution for different values of the engine characteristics slope and different initial rotor velocities



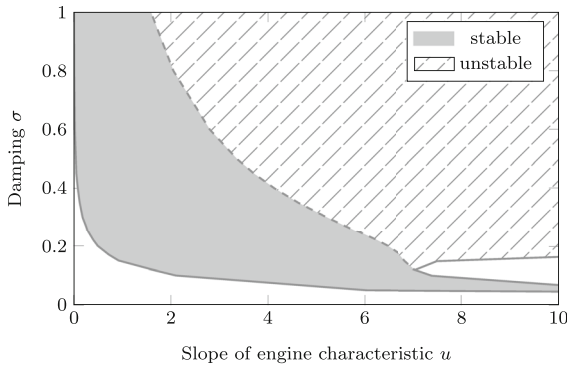


Fig. 9 Existence and stability areas of the periodic solution

tion (CS), and the white areas correspond to the attraction area of the resonance solution (RS).

Three parameter configurations are considered: one where the stationary resonance solution (RL) exists ($u = 1.5$, see the left-hand column of the diagrams) and two with the periodic resonance solution ($u = 5$, see the middle column of the diagrams and $u = 7$, see the right-hand column of the diagrams). For small values of engine parameter u , it is possible to realize a compensating solution while accelerating the rotor from its rest position only within a small range of initial balancing pendulum positions (see Fig. 8a). An increase in parameter value u , corresponding to an increase in engine power, leads to an extension of the attraction area of the compensating solution (compare Fig. 8b and c).

In all three cases considered, increasing the initial rotor speed in the undercritical region ($\bar{\omega}_0 < 1$) does not significantly extend the region of attraction of the compensating solution, but the region rotates about the rotor axis in the direction of the phase flow (see Figs. 8a–f and 7). When the rotor starts in the supercritical region ($\bar{\omega}_0 > 1$), an increase in the initial rotor speed leads to a rapid increase in the region of attraction of the compensating solution. However, even in the case of an initial rotor speed corresponding to the nominal engine speed, small areas of attraction of the resonant solutions remain (see Fig. 8m–o).

7 Periodic resonance solution stability

Unlike the vibration exciter, the periodic resonance solution in self-balancing systems can become unstable. To assess the stability of the periodic solution

$\bar{\omega} = \Omega^*(\phi)$, $\bar{\psi} = \Psi^*(\phi)$, $\bar{\delta} = 0$ Eqs. (41)–(43) are linearized near this periodic solution. The result is a system of linear differential equations with periodic coefficients of the following structure:

$$\Delta \bar{\omega}' = \left. \frac{dF_\omega}{d\bar{\omega}} \right|_{\bar{\omega}=\omega^*, \bar{\psi}=\psi^*, \bar{\delta}=0} \Delta \bar{\omega} + \left. \frac{dF_\omega}{d\bar{\psi}} \right|_{\bar{\omega}=\omega^*, \bar{\psi}=\psi^*, \bar{\delta}=0} \Delta \bar{\psi}, \tag{56}$$

$$\Delta \bar{\psi}' = \left. \frac{dF_\psi}{d\bar{\psi}} \right|_{\bar{\omega}=\omega^*, \bar{\psi}=\psi^*, \bar{\delta}=0} \Delta \bar{\psi} + \left. \frac{dF_\psi}{d\bar{\omega}} \right|_{\bar{\omega}=\omega^*, \bar{\psi}=\psi^*, \bar{\delta}=0} \Delta \bar{\omega}, \tag{57}$$

$$\Delta \bar{\delta}' = \left. \frac{dF_\delta}{d\bar{\delta}} \right|_{\bar{\omega}=\omega^*, \bar{\psi}=\psi^*, \bar{\delta}=0} \Delta \bar{\delta}, \tag{58}$$

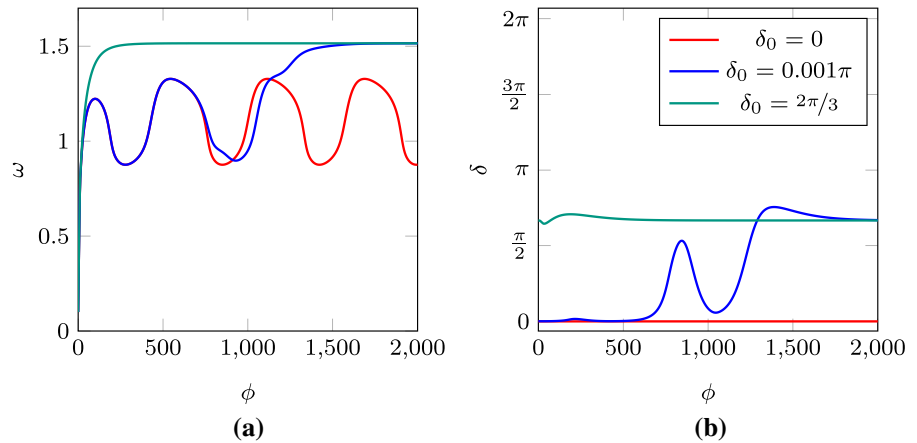
where F_ω , F_ψ and F_δ are the right-hand sides of Eqs. (41), (42) and (43), respectively. It is important to note that Eq. (58), which describes the angle between the pendulum balancers near the periodic solution, is completely decoupled from Eqs. (56) and (57). From the numerical calculation of the Floquet multipliers, it follows that the periodic solution stability is determined alone by the stability of the solution to this equation. Therefore, only this Floquet multiplier needs to be calculated to estimate the stability. The areas of existence and system periodic resonance solution stability are shown in Fig. 9. The area filled in gray corresponds to the periodic resonant solution stability region. In the cross shaded area, the periodic resonance solution is unstable. In the unshaded (white) regions, the periodic resonance solution does not exist.

The system behavior during acceleration in the case of an unstable periodic solution is shown in Fig. 10. A small deviation in the initial conditions from $\delta_0 = 0$ leads to an increasing angle between the pendulum balancers (see the red line in Fig. 10b). The rotor speed can remain close to the resonance solution for a long time until the angle between the pendulums reaches a critical value, after which the system quickly reaches a stable compensating solution (see the blue line in Fig. 10a).

8 Conclusions

The slow dynamics of self-balancing systems while passing through resonance were investigated using the

Fig. 10 Evaluation of the rotor rotation speed ω (a) and the angle δ between the pendulums (b) for different initial values of angle δ between the pendulums in the case of an unstable periodic solution ($u = 8$, $\sigma = 0.2$)



averaging method for partially strongly damped systems. Thus, the description of the system with four degrees of freedom was reduced to only three differential equations of the first order. Both types of capture into resonance typical for the vibration exciter with two coaxial imbalances were also found in the self-balancing system. In contrast to the vibration exciter, the periodic solution, which corresponds to nonstationary capture into resonance and is characterized by a very slow modulation of the rotor speed, can become unstable in self-balancing systems at sufficiently high values of the engine characteristic slope and damping in the oscillating part of the system. In the considered case, both resonant solutions coexist with an overcritical solution, which provides full compensation for the system imbalance. Whether the system passes through or is caught into resonance is highly dependent on the initial conditions. In the case of low values of the engine characteristic slope, the attraction area of the compensating solution is negligibly small and increases with the engine power.

Further investigations will be focused on the experimental verification of the obtained results alongside with possible generalizations for various exciters [3, 10] including self-synchronization concepts [1].

Author contributions All authors contributed to the study conception and design. Methodology and supervision were performed by Alexander Fidlin. Material preparation, data collection and analysis were performed by Olga Drozdetskaya. The first draft of the manuscript was written by Olga Drozdetskaya, and all authors commented on previous versions of the manuscript. All authors read and approved the final manuscript.

Funding Open Access funding enabled and organized by Projekt DEAL.

Availability of data and material The datasets generated during and/or analyzed during the current study are available from the corresponding author on reasonable request

Declarations

Conflict of interest The authors declare that there is no conflict of interest

Code availability Not applicable.

Open Access This article is licensed under a Creative Commons Attribution 4.0 International License, which permits use, sharing, adaptation, distribution and reproduction in any medium or format, as long as you give appropriate credit to the original author(s) and the source, provide a link to the Creative Commons licence, and indicate if changes were made. The images or other third party material in this article are included in the article's Creative Commons licence, unless indicated otherwise in a credit line to the material. If material is not included in the article's Creative Commons licence and your intended use is not permitted by statutory regulation or exceeds the permitted use, you will need to obtain permission directly from the copyright holder. To view a copy of this licence, visit <http://creativecommons.org/licenses/by/4.0/>.

References

1. Blekhman, I.I.: Synchronization in science and technology. ASME Press translations. ASME Press, New York (1988). <https://books.google.de/books?id=ao1QAAAAMAAJ>
2. Drozdetskaya, O., Fidlin, A.: On the passing through resonance of a centrifugal exciter with two coaxial unbalances. *Eur. J. Mech. A/Solids* **72**, 516–520 (2018)
3. Fidlin, A., Drozdetskaya, O.: On the averaging in strongly damped systems: the general approach and its application to asymptotic analysis of the Sommerfeld effect. *Procedia IUTAM* **19**, 43–52 (2016)

4. Fidlin, A., Thomsen, J.J.: Non-trivial effects of high-frequency excitation for strongly damped mechanical systems. *Int. J. Non-Linear Mech.* (2008)
5. Green, K., Champneys, A.R., Friswell, M.I.: Analysis of the transient response of an automatic dynamic balancer for eccentric rotors. *Int. J. Mech. Sci.* **48**(3), 274–293 (2006)
6. Green, K., Champneys, A.R., Lieven, N.J.: Bifurcation analysis of an automatic dynamic balancing mechanism for eccentric rotors. *J. Sound Vib.* **291**, 861–881 (2006)
7. Horvath, R., Flowers, G.T., Fausz, J.: Influence of nonlinearities on the performance of a self-balancing rotor system. In: *ASME International Mechanical Engineering Congress and Exposition*. Orlando, Florida USA (2005)
8. Hwang, C.H., Chung, J.: Dynamic analysis of an automatic ball balancer with double races. *JSME Int. J. Ser. C Mech. Syst. Mach. Elements Manuf.* **42**(2), 265–272 (1999)
9. Ishida, Y.: Recent development of the passive vibration control method. *Mech. Syst. Signal Process.* **29**, 2–18 (2012)
10. Miklós, A., Szabó, Z.: Simulation and experimental validation of the dynamical model of a dual-rotor vibrotactor. *J. Sound Vib.* **334**, 98–107 (2015)
11. Rajalingham, C., Bhat, R.B.: Complete balancing of a disk mounted on a vertical cantilever shaft using a two ball automatic balancer. *J. Sound Vib.* **290**(1–2), 169–191 (2006)
12. Rodrigues, D.J., Champneys, A.R., Friswell, M.I., Wilson, R.E.: Automatic two-plane balancing for rigid rotors. *Int. J. Non-Linear Mech.* **43**(6), 527–541 (2008)
13. Ryzhik, B., Sperling, L., Duckstein, H.: Non-synchronous motions near critical speeds in a single-plane auto-balancing device. *Technische Mechanik. Sci. J. Fundament. Appl. Eng. Mech.* **24**(1), 25–36 (2004)
14. Sperling, L., Ryzhik, B., Duckstein, H.: Single-plane auto-balancing of rigid rotors. *Technische Mechanik* **24**, 1–24 (2004)
15. Thearle, E.L.: A new type of dynamic-balancing machine. *Trans. ASME* **54**(12), 456–465 (1932)

Publisher's Note Springer Nature remains neutral with regard to jurisdictional claims in published maps and institutional affiliations.